

# Development of ~~the a~~ micro-~~pixel~~ chamber based on MEMS technology

T. Takemura<sup>1</sup>, A. Takada<sup>1</sup>, T. Kishimoto<sup>1</sup>, S. Komura<sup>1</sup>, H. Kubo<sup>1</sup>, Y. Matsuoka<sup>1</sup>, K. Miuchi<sup>2</sup>, S. Miyamoto<sup>1</sup>, T.

Mizumoto<sup>1</sup>, Y. Mizumura<sup>1</sup>, T. Motomura<sup>4</sup>, Y. Nakamasu<sup>1</sup>, K. Nakamura<sup>1</sup>, M. Oda<sup>1</sup>, K. Ohta<sup>4</sup>, J. D. Parker<sup>1</sup>, T.

Sawano<sup>3</sup>, S. Sonoda<sup>1</sup>, T. Tanimori<sup>1</sup>, D. Tomono<sup>1</sup>, and K. Yoshikawa<sup>1</sup>

<sup>1</sup> Kyoto University, Japan <sup>2</sup>Kobe University, Japan <sup>3</sup>Kanazawa University, Japan <sup>4</sup>Dai Nippon Printing Co., Ltd.

**Abstract.** A micro-pixel chamber ~~called  $\mu$ -PIC~~ is our original gaseous two-dimensional imaging detectors originally manufactured by using Printed-printed Circuit-circuit Board-board (PCB) technology. ~~It is using~~ They are used in MeV gamma-ray astronomy, medical-imaging, neutron imaging, ~~the search for~~ dark matter-search and dose monitoring. ~~A-The~~ position resolution of the present  $\mu$ -PIC is ~~approximately~~ 120  $\mu$ m (RMS); however, ~~some the~~ applications require a fine position resolution of less than 100  $\mu$ m. ~~For this purpose~~ To this end, we have started to develop a  $\mu$ -PIC based on Micro-microElectro-Mmechanical System-system (MEMS) technology, which provides better manufacturing accuracy than PCB technology. ~~The Our~~ simulation ~~expected-predicted that~~ the gains of MEMS  $\mu$ -PICs ~~are to be~~ twice ~~higher-than-that-those~~ of PCB  $\mu$ -PICs at the same anode voltage. We manufactured two MEMS  $\mu$ -PICs and tested them ~~in order~~ to study their behavior ~~of~~ MEMS  $\mu$ -PICs. In these experiments, we ~~succeeded to successfully~~ operated the fabricated MEMS  $\mu$ -PICs; ~~we and we obtained-achieved~~ a maximum gain of ~~approximately~~  $5 \times 10^3$  and collected their energy spectra under the irradiation of X-rays from  $^{55}\text{Fe}$ . However, the measured gains of the MEMS  $\mu$ -PICs ~~are were less lower~~ than half of the values predicted in the simulated gains. We ~~consider-postulated~~ that the gains of the MEMS  $\mu$ -PICs ~~reduce due to are diminished by~~ the effect of the silicon used as a semiconducting substrate.

KEYWORDS: gaseous detector, Micro-pattern detector, Micro Electro Mechanical System

## 1 Introduction

A micro-pixel chamber ~~called  $\mu$ -PIC~~ [1] is a gaseous two-dimensional imaging detector (Figure 1 ~~shows the schematic view of a  $\mu$ -PIC~~). Each pixel of the  $\mu$ -PIC, ~~which~~ has an anode ~~via~~ with a diameter of 60  $\mu$ m and a cathode ~~electrode~~ with a hole diameter of 250  $\mu$ m ~~and~~ is ~~placed-positioned~~ with a pitch of 400  $\mu$ m. A gas avalanche occurs near the anode ~~via due to because of~~ the strong electric field between these electrodes; therefore, each pixel ~~works-functions~~ as a proportional counter. The a ~~node-via~~ are connected to an anode strip electrode on the back of the substrate, and the cathodes ~~is are~~ formed in strip electrodes on the front surface. A ~~Two-dimensional~~

### Comment [Editor1]: Tip: Serial comma

In American English, a comma (called serial or oxford comma) is inserted before “and” in a series.

### Comment [Editor2]: Tip: Scientific notation and convention

Use a multiplication sign ( $\times$ ) instead of the letter x to at such instances. Note that a space should be inserted before and after the sign.

readout ~~is available~~ can be fabricated using anode and cathode strips arranged orthogonally. ~~A  $\mu$ -PICs are~~ manufactured by ~~PCB (Printed Circuit Board) (PCB)~~ technology and ~~is are~~ composed of copper electrodes and ~~100- $\mu$ m-thick~~ polyimide substrates ~~with the thickness of 100- $\mu$ m~~. PCB technology ~~allows us to enable~~ the low-cost manufacturing ~~cheaply of a~~ large-area  $\mu$ -PICs (10  $\times$  10 cm<sup>2</sup> [2] or 30  $\times$  30 cm<sup>2</sup> [3]). ~~The PCB  $\mu$ -PICs feature~~ has a fine position resolution (RMS, [3.1 [JP] 省略形の表記をご確認ください]  $\approx$  120  $\mu$ m) [4], a high gas gain (nominal 6000, maximum 15,000) [5], and ~~a~~ good gain uniformity (RMS  $\approx$  5%). ~~The PCB  $\mu$ -PICs is~~ have been used in a wide range of applications including ~~applied in a wide field, for example,~~ MeV gamma-ray astronomy [6], medical imaging [7], ~~the search for~~ dark matter ~~search~~ [8], neutron imaging [9], and dose monitoring [10]. ~~However, n~~ Neutron imaging applications require a position resolution ~~of~~ less than 100  $\mu$ m

**Comment [Editor3]:** Remark: Please check if the edit retains the intended meaning.

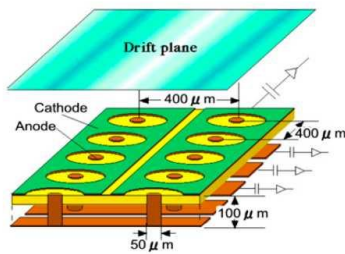


**Figure 1.** Schematic ~~view~~ of a  $\mu$ -PIC based on PCB technology [1]. The  $\mu$ -PIC is composed of copper electrodes and ~~a 100- $\mu$ m~~ poly-imide substrate ~~of 100- $\mu$ m~~. Each pixel of the  $\mu$ -PIC, ~~which~~ has an anode ~~via~~ with a diameter of 60  $\mu$ m and a cathode ~~electrode~~ with a hole diameter of 250  $\mu$ m ~~and~~, is ~~placed~~ ~~fabricated~~ with a pitch of 400  $\mu$ m. A gas avalanche occurs near the anodes ~~via due to because of~~ the strong electric field between these electrodes; therefore, each pixels ~~functions works~~ as a proportional counter.

**Comment [Editor4]:** Remark: Please check if the edit retains the intended meaning.

and MeV gamma-ray astronomy requires precise tracking of charged particles with an angular resolution ~~of~~ less than 5° ~~degrees~~. ~~For this~~ Satisfying these requirements ~~aim, we need to~~ necessitates the development of a  $\mu$ -PIC with a fine position resolution.

Because of the ~~limitations of the~~ manufacturing accuracy of PCB technology, the diameter of  $\mu$ -PIC anodes ~~via~~ is limited to ~~approximately~~ 50  $\mu$ m.



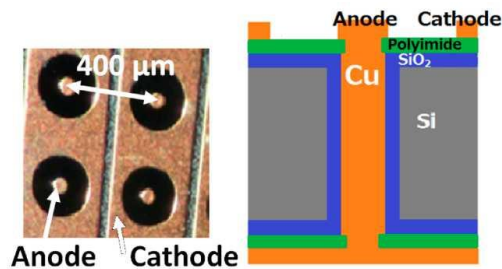


**Figure 2.** A photograph (left) and a schematic view of the cross-

section (right) of a MEMS  $\mu$ -PIC. A-The substrate of the MEMS  $\mu$ -PIC.

is composed of a silicon layer with the a thickness of 400  $\mu$ m, a thin SiO<sub>2</sub> layer, and a thin polyimide layer. The thin SiO<sub>2</sub> layer and polyimide layers are insulated on the MEMS  $\mu$ -PIC for to enhance the discharge tolerance.

**Comment [Editor5]:** Remark: Please check if the edit retains the intended meaning.

Therefore, we need other a more advanced technology is needed technology for manufacturing a fine-pitch  $\mu$ -PICs. Micro-Electro-Mechanical System-system (MEMS) technology is one such of such expecting capable technologies. Recently, the MEMS technology is well established, and the MEMS manufacturing costs have been reduced to similar levels similar to that of those of PCB technology. Additionally In addition, MEMS technology enables us to the use the of thicker substrates than compared with those for PCB technology. In the case of  $\mu$ -PICs, the gain depends on the thickness of the substrate: a The two two-times fold thicker substrate improves the gain to by a factor of two [11]. Thus, a MEMS  $\mu$ -PIC is expected to have exhibit a fine position resolution and a high gas gain. However, the substrates used in of MEMS technology is composed comprise of silicon, which is a semiconductor; thus, so that we need to investigate the effect of the difference between a semiconducting or substrate being substituted for and the insulating substrate of  $\mu$ -PICs should be investigated or. In this work, we We manufactured two MEMS  $\mu$ -PICs in order to study investigate their behavior. Here, we report the results of both the simulations and the first measurements experiments.

## 2 Simulation study of MEMS $\mu$ -PIC

We made-fabricated a MEMS  $\mu$ -PIC which is similar to the with a structure similar to that of a PCB  $\mu$ -PIC in order to focus on the effect of the difference between using a semiconductor instead of and an insulating substrate. Figure 2 shows a photo and a schematic view of the cross-section of the manufactured MEMS  $\mu$ -PIC. The differences between a PCB  $\mu$ -PIC and a MEMS  $\mu$ -PIC are lie in the substrate material and its thickness of the substrate, which are listed in Table 1. For simulation purposes, the substrate of MEMS  $\mu$ -PIC substrate is was assumed to comprised of a 400- $\mu$ m-thick silicon layer with the thickness of 400  $\mu$ m, a thin SiO<sub>2</sub> layer, and a thin polyimide layer in contrast to that of; by contrast, the PCB  $\mu$ -PIC substrate was assumed to is composed of a polyimide layer with the a thickness of 100  $\mu$ m. The thin SiO<sub>2</sub> layer and polyimide layer are insulated on MEMS  $\mu$ -PICs for to enhance their the discharge tolerance. We varied the thickness of the SiO<sub>2</sub> layer in t the manufactured MEMS  $\mu$ -PICs are different in the thickness of SiO<sub>2</sub> layer in order to study the effect of its effects on device performance SiO<sub>2</sub> layer. Other parameters (such as the thickness of the strips, the pitches of pixels, the diameter of the cathode hole, the diameter of the anode via, and the width of a the cathode strip) is almost were approximately the same.

**Comment [Editor6]:** Remark: Please check if the edit retains the intended meaning.

We evaluated the geometries of the PCB and MEMS  $\mu$ -PICs in order to study their gains of PCB and MEMS  $\mu$ -PICs. We

**Table 1.** Thickness and relative permittivity values used in simulations of each layers in the  $\mu$ -PICs.

material	relative permittivity	MEMS [ $\mu$ m]	PCB [ $\mu$ m]
copper electrode	10 <sup>10</sup>	15	15
polyimide	3.2	4	~100
silicon	11	400	—
SiO <sub>2</sub>	4.5	1 or 10	—

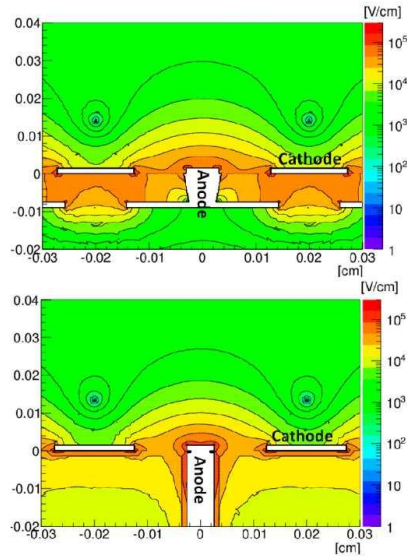


**Figure 3.** Electric fields of the cross section of a PCB  $\mu$ -PIC and a MEMS  $\mu$ -PIC calculated using the program Elmer in for the case of an anode voltage of 460 V. The drift electric field and cathode voltage were fixed at 1.0 kV/cm and 0 V, respectively.

fabricated a  $\mu$ -PIC pixel electrodes using the Gmsh program [12] and calculated the electric field around the  $\mu$ -PICs using the Elmer program [13]. We simulated the avalanche and obtained gas gains using the Garfield++ program with the a three-dimensional mesh [14]. We used the a gas of Ar/C<sub>2</sub>H<sub>6</sub> (pressure ratio 90:10) at 1 atm and adopted a penning-effect rate of 0.31 [15]. The drift electric field and cathode voltage were fixed at 1.0 kV/cm and 0 V, respectively. Figure 3 shows the electric fields of the cross sections of the PCB  $\mu$ -PIC and MEMS  $\mu$ -PIC in for the case of an anode voltage of 460 V. The electric field at 1  $\mu$ m above the edge of the anode was 1.7  $\times 10^5$  V/cm for the PCB  $\mu$ -PIC and 2.2  $\times 10^5$  V/cm for the MEMS  $\mu$ -PIC. The thick substrate of the MEMS  $\mu$ -PIC concentrates the electric field lines to an anode, because the thick substrate obstructs the electric field lines between the cathode strip and the anode strips. Therefore, the MEMS  $\mu$ -PIC has exhibits a stronger electric field. The dependence of the simulated avalanche size of dependence on the anode voltage is shown in Figure 4. In this figure, the dashed and solid lines represent the simulated gains of the PCB [16] and MEMS  $\mu$ -PICs, respectively. The measured gains of the PCB  $\mu$ -PICs are excellent agreement agree well with the simulated gains [16]; there we

**Comment [Editor7]:** Remark: Please check if the edit retains the intended meaning.



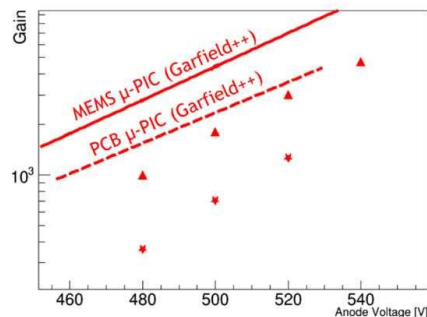


**Figure 4.** The simulated and measured gains of PCB and MEMS  $\mu$ -PICs. The dashed and solid lines represent the simulated gains of a PCB  $\mu$ -PIC and a MEMS  $\mu$ -PIC, respectively. The simulation expected-predicted that the gains of the MEMS  $\mu$ -PIC are twice higher than that to be twice those of the PCB  $\mu$ -PIC in the situation at the of same anode voltage. Stars and triangles represent the measured gains of the MEMS  $\mu$ -PIC with 1- $\mu$ m and 10-10- $\mu$ m  $\text{SiO}_2$  layers, respectively. The gains are were measured using in the setup shown in of Figure 5.

fore it is therefore considered that Garfield++ to be is a reliable simulator in avalanche around a  $\mu$ -PIC. The simulation expected-predicted that the gains of the MEMS  $\mu$ -PIC are twice to be twice those higher than that of the PCB  $\mu$ -PIC in the situation of at the same anode voltage. In additionally, we studied the effect of the  $\text{SiO}_2$  layer in the simulation, so and observed that the gains of the MEMS  $\mu$ -PIC has no dependence were independent of on the thickness of the  $\text{SiO}_2$  layer when the layer thickness was less than 15  $\mu$ m.

### 3 Measurements of the gas gains of MEMS

#### $\mu$ -PICs

For confirming of To confirm the simulation results, we operated the manufactured MEMS  $\mu$ -PICs for the first time with using the setup shown in Figure 5. The active area of the MEMS  $\mu$ -PIC is was 5  $\times$  10 mm<sup>2</sup>, and it has comprised 6 cathode and 10 anode strips. The MEMS  $\mu$ -PIC was set placed in a sealed aluminum vessel filled with a normal pressure Ar/ $\text{C}_2\text{H}_6$  gas (the in a pressure ratio of 90:10) at atmospheric pressure. We placed positioned a gas electron multiplier (GEM) [17] at 3 mm above the  $\mu$ -PIC. The GEM has a polyimide substrate with a thickness of

**Comment [Editor8]:** Remark: Please check if the edit retains the intended meaning.

100  $\mu\text{m}$ , and its hole diameters is 70  $\mu\text{m}$  with a pitch of 140  $\mu\text{m}$ ; and the active area of the GEM is  $10 \times 10 \text{ cm}^2$ . We operated the GEM with a gain of approximately 20, and the electric field of the induction field was 1 kV/cm. The drift plane was placed at 3 mm above the GEM, and the electric field of 250 V/cm was applied in the drift space. Therefore, the volume of the detection space was  $5 \times 10 \times 3 \text{ mm}^3$ ; this space is indicated with the hatched area in Figure 5. The signals from anode and cathode strips are read out by a CMOS ASIC chip [18]. This ASIC has 16 analog input channels, 16 digital output channels, and an analog sum signal. The analog sum signal is fed to an 8-bit FADC (3.1 [JP] 省略形の表記をご確認ください) operated at 25-25-MHz clocks. The details of the data acquisition system of used in these experiments is have been described in T. Mizumoto elsewhere [18].

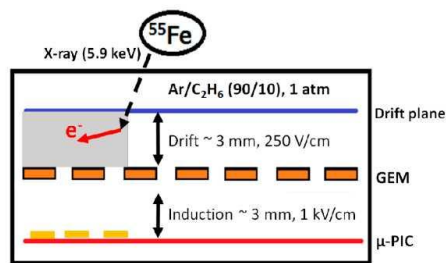


Figure 5. Schematic view of the setup of the test operation. The details are described in the text.

At first, we first operated the MEMS  $\mu\text{-PIC}$  having the  $\text{SiO}_2$  layer with thickness of a 10-10- $\mu\text{m}$   $\text{SiO}_2$  layer under the irradiation of 5.9 keV X-rays from  $^{55}\text{Fe}$ . Figure 6 shows the signal when the anode voltage is was 460 V. The MEMS  $\mu\text{-PIC}$  was stably operated with at a discharge rate of less than 0.03 Hz and at the an anode voltage of 560 V. In the case of the MEMS  $\mu\text{-PIC}$  having the  $\text{SiO}_2$  layer with thickness with a of 1-1- $\mu\text{m}$ -thick  $\text{SiO}_2$  layer, the leak current was approximately 160 nA when we applied an under the applied anode voltage and the leak current remained greater than over 20 nA for lasted during longer than 4 hours. The discharge rate of (The MEMS  $\mu\text{-PIC}$  with a 1-1- $\mu\text{m}$ -thick  $\text{SiO}_2$  layer layer had the discharge rate was greater more than 0.5 Hz at the an anode voltage of 530 V. Therefore, an  $\text{SiO}_2$  layer is essential to for the its stable operation.

**Comment [Editor9]:** Remark: Please check if the edit retains the intended meaning.

Figure 7-(a) and (b) show the ~~energy spectra of  $^{55}\text{Fe}$~~  energy spectra of a-PCB ~~/PIC~~ (25  $\times$  25 mm<sup>2</sup>) and a-MEMS  $\mu$ -PICs, respectively. The energy resolution of the PCB  $\mu$ -PIC at 5.9 keV ~~is was~~ 40-%, with the ~~a~~ gain of  $1.1 \times 10^3$ ; ~~by contrast, whereas~~, the energy resolution of the MEMS  $\mu$ -PIC (4-1- $\mu\text{m}$ -thick SiO<sub>2</sub> layer) at 5.9 keV ~~is was~~ 57-%, with the ~~a~~ gain of  $1.2 \times 10^3$ . The energy resolution of

the MEMS  $\mu$ -PIC (40-10- $\mu\text{m}$ -thick SiO<sub>2</sub> layer) ~~is was~~ nearly equal to that of the MEMS  $\mu$ -PIC (4-1- $\mu\text{m}$ -thick SiO<sub>2</sub> layer). The detection area of the MEMS  $\mu$ -PIC was ~~one-tenth~~ 10% smaller than that of the PCB  $\mu$ -PIC. Electrons escape from the detection area of the MEMS  $\mu$ -PIC more easily; thus, most of the electrons deposit partial energy. ~~Therefore, we consider that~~ the energy resolution of the MEMS  $\mu$ -PIC eventually became worse than that of the PCB  $\mu$ -PIC. ~~In future experiments, w~~We plan to obtain the energy spectrum with imaging for the rejection of escape electrons, after we achieve a stable operation with a gain of  $10^4$ .

**Comment [Editor10]:** Remark: Please check if the edit retains the intended meaning.

In Figure 4, stars and triangles represent the measured gains of MEMS  $\mu$ -PICs with 1  $\mu\text{m}$ - and 10  $\mu\text{m}$ -thick SiO<sub>2</sub> layers, respectively. The maximum gain of the MEMS  $\mu$ -PIC ~~achieved-reached~~ approximately  $5 \times 10^3$ . The gains of the MEMS  $\mu$ -PICs ~~of-with~~ 4-1- $\mu\text{m}$ - and 40-10- $\mu\text{m}$ -thick SiO<sub>2</sub> layers ~~are were~~ 16-% and 40-% ~~that~~ of the simulated gains at ~~anthe~~ anode voltage of 500 V, respectively. Because a-semiconductors ~~contain-had~~ charge carriers, the silicon near the anodes and cathodes became negatively and positively charged, respectively; ~~when-we~~under an applied ~~the~~ anode voltage. ~~Our-However, our~~ simulations with the Elmer and Garfield++ programs did not ~~consider~~ account for such an effect. The electric field around the anode ~~via~~ would be weaker than ~~that predicted by the~~ simulated ~~expectation-by~~ions because of the charge-up effect of silicon; therefore, the gains of the MEMS  $\mu$ -PIC ~~were~~ reduced. ~~Besides~~In addition, the measured gas gain depend~~ed~~ on the thickness of the SiO<sub>2</sub> layer, which ~~was served as an~~

**Comment [Editor11]:** Remark: Please note that this sentence repeats information in the figure caption. Please consider deleting it and adding an introductory phrase such as "As shown in Figure 4..." to the next sentence.

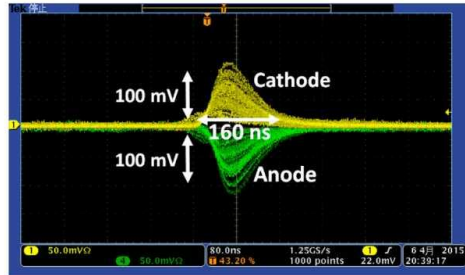


**Figure 6.** The signals of MEMS  $\mu$ -PIC with  $\text{SiO}_2$  layer of 10  $\mu\text{m}$  by the 5.9 keV X-ray of  $^{55}\text{Fe}$  source. Positive and negative signals are obtained from cathodes and anodes, respectively. Voltage between gem-GEM top and bottom is 320 V, and anode voltage is 460 V. The filled gas is with a normal-pressure  $\text{Ar}/\text{C}_2\text{H}_6$  (pressure ratio 90:10) gas mixture.

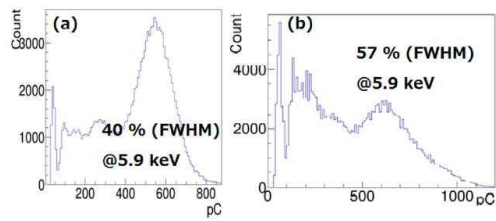


**Figure 7.** The energy spectrum of the 5.9 keV X-ray of  $^{55}\text{Fe}$  source PCB  $\mu$ -PIC (a) and (b), respectively.

insulator placed-positioned between the electrodes and the silicon substrate. As described in the-section 2, the simulated gain had no relation to is independent of the thickness of the  $\text{SiO}_2$  layer; however, a-The thinner  $\text{SiO}_2$  layer results in is, the more strongly the chara greater chargingge-up effect appeared. The leak current during start-up is the-additional evidence of the charge-upthis charging effect. To realize-achieve both the-stable operation and the-a high gain of-with a MEMS  $\mu$ -PIC, we need to reduce the charge-uping effect of the silicon. We considered two solutions toof this issue. One is to fabricate a MEMS  $\mu$ -PIC with-using atthe glass substrate which-that contains no semiconductor. We can manufacture a MEMS μ-PIC with-on atthe glass substrate, but the cost will be doing so is

expensive. ~~Another~~ The other solution is ~~the~~ to fabricate a MEMS  $\mu$ -PIC with ~~the a~~ thick  $\text{SiO}_2$  layer. We believe that we can ~~manufacture-fabricate~~ a MEMS  $\mu$ -PIC ~~having the~~ with a  $\text{SiO}_2$  layer ~~with the thickness of 15–30–30- $\mu\text{m}$~~  thick, and we plan to manufacture them in the future. ~~When we realize these~~ We expect that the resulting MEMS  $\mu$ -PIC, MEMS / PICs ~~will will have~~ be useful-high activities in various applications.

**Comment [Editor12]:** Remark: Please note that if you have actually reported manufacturing such a  $\mu$ -PIC, please consider adding a citation to your previous work.

**Comment [Editor13]:** Remark: Please check if the edit retains the intended meaning.

## 4 Summary

The applications of  $\mu$ -PICs require a finer position resolution than that of current PCB  $\mu$ -PICs. To satisfy this ~~request~~requirement, we ~~manufactured-fabricated~~ and studied ~~the~~ MEMS  $\mu$ -PICs. Specifically, ~~we~~ We made ~~fabricated a~~ MEMS  $\mu$ -PICs ~~which with a structure is~~ similar to ~~that of the structure of~~ a PCB  $\mu$ -PIC in order to focus on the effects of ~~the difference between using a~~ semiconducting ~~ingor and~~ instead of ~~a-an~~ insulating substrate~~or~~. The ~~S~~simulations ~~expected-predicted that~~ the gains of the MEMS  $\mu$ -PICs ~~are to be twice higher than that~~ twice those of PCB  $\mu$ -PICs ~~in the situation of at the~~ same anode voltage. The MEMS  $\mu$ -PIC with a ~~1–1- $\mu\text{m}$ -thick~~  $\text{SiO}_2$  layer ~~is~~ was unstable, ~~and this result shows~~ demonstrating that an  $\text{SiO}_2$  layer is essential to the stable operation of MEMS  $\mu$ -PICs. For the first time, we successfully obtained ~~the a~~ signal and ~~the~~ energy spectra using MEMS  $\mu$ -PICs ~~with~~ under ~~the~~ irradiation of X-ray-rays from  $^{55}\text{Fe}$ . The maximum gain of ~~the~~ MEMS  $\mu$ -PICs ~~achieved-reached~~ approximately  $5 \times 10^3$ . However, the gains measured ~~gains at an anode voltage of 500 V are were~~ 16%–40% that of ~~the~~ simulated ~~gains values at the anode voltage of 500 V~~. We considered ~~ed~~ that the gains of ~~the~~ MEMS  $\mu$ -PICs ~~reduce due to were~~ diminished by the effect of ~~the semiconducting~~ silicon ~~substrate as a semiconductor~~. To ~~reduce~~ minimize the effect of the semiconductor, we ~~will plan to~~ manufacture ~~the~~ MEMS  $\mu$ -PICs with thicker  $\text{SiO}_2$  layers or ~~with the~~ glass substrates.

## Acknowledgements

This work was supported by the "UCHUGAKU" project of the Unit of Synergetic Studies for Space, Kyoto University.

## References

- [1] A. Ochi, et al., Nuclear Instruments and Methods in Physics Research Section A 471, 264-276 (2001).
- [2] H. Kubo, et al., Nuclear Instruments and Methods in Physics Research Section A 513, 94-98 (2003).
- [3] A. Takada, et al., Nuclear Instruments and Methods in Physics Research Section A 573, 195-199 (2007).
- [4] T. Nagayoshi, et al., Nuclear Instruments and Methods in Physics Research Section A 525, 20-27 (2004).
- [5] K. Miuchi, et al., IEEE Transactions on Nuclear Science 50, 825-830 (2003).
- [6] T. Tanimori, et al., The Astrophysical Journal 810, 28 (2015).
- [7] S. Kabuki, et al., Nuclear Instruments and Methods in Physics Research Section A 623, 606-607 (2010).
- [8] K. Nakamura, et al., Progress of Theoretical and Experimental Physics, 043F01 (2015).
- [9] J. D. Parker, et al., Nuclear Instruments and Methods in Physics Research Section A 697, 23-31 (2013).
- [10] T. Mizumoto, et al., Journal of Instrumentation 10, C06003 (2015).
- [11] T. Nagayoshi, et al., Nuclear Instruments and Methods in Physics Research Section A 546, 457-465 (2005).
- [12] <http://geuz.org/gmsh>.
- [13] <http://www.csc.fi/english/pages/elmer>.
- [14] <http://garfieldpp.web.cern.ch/garfieldpp>.
- [15] O. Sahin, et al., Journal of Instrumentation 5, P05002 (2010).
- [16] A. Takada, et al., Journal of Instrumentation 8, C10023 (2013).
- [17] F. Sauli, Nuclear Instruments and Methods in Physics Research Section A 386, 531-534 (1997).
- [18] T. Mizumoto, et al., Nuclear Instruments and Methods in Physics Research Section A 800, 40-50 (2015).

????????

